

## Research Paper

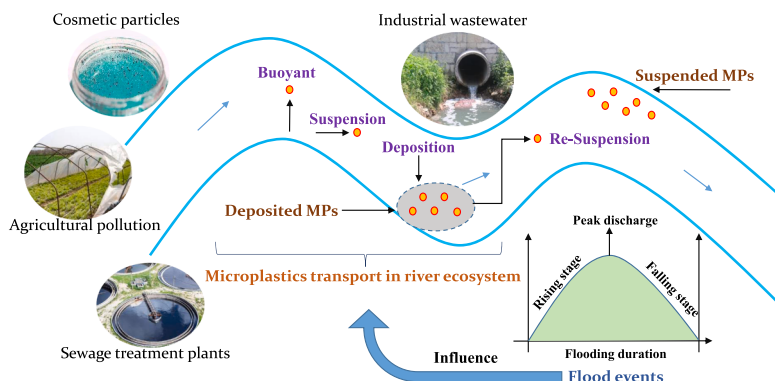
## Dispersal and transport of microplastic particles under different flow conditions in riverine ecosystem

Xiaorong Lu <sup>a,c</sup>, Xuelei Wang <sup>a,\*</sup>, Xi Liu <sup>b</sup>, Vijay P. Singh <sup>c</sup><sup>a</sup> Key Laboratory for Environment and Disaster Monitoring and Evaluation of Hubei, Innovation Academy for Precision Measurement Science and Technology, Chinese Academy of Sciences, Wuhan 430077, China<sup>b</sup> Ecological Environment Monitoring and Scientific Research Center, Yangtze River Basin Ecological Environment Supervision and Administration Bureau, Ministry of Ecological Environment, Wuhan 430010, China<sup>c</sup> Department of Biological and Agricultural Engineering & Zachry Department of Civil Engineering, Texas A&M University, College Station, TX 77843-2117, USA

## HIGHLIGHTS

- Dispersal and transport of microplastic particles in riverine ecosystem.
- Effect of different rainfall intensity on microplastics transport.
- Differences in dispersal and transport pattern among MP types.
- Temporal and spatial characteristics of microplastics concentration.

## GRAPHICAL ABSTRACT



## ARTICLE INFO

Editor: Dr. R Teresa

## Keywords:

Microplastics transport  
Hydrodynamic simulation  
Particle tracking  
Riverine ecosystem

## ABSTRACT

Microplastic (MP) pollution is a global issue owing to its potential threats to ecosystems and human health. MP pollution in river ecosystems is widely investigated, but the transport process under different hydrological conditions remain unclear. In this study, an approach of particle tracking in conjunction with hydrodynamic modeling was developed to investigate the dispersal and transport processes of microplastic particles in riverine ecosystem. The concentration and dispersal pattern of polyamide (PA), polyethylene (PE), polypropylene (PP), polystyrene (PS), and polyethylene terephthalate (PET) particles under base flow and flood events with recurrence intervals of 10-year, 20-year and 50-year were identified. Results indicated that rainfall intensity had a significant impact on the microplastic transport in rivers. Higher suspension concentration and lower sedimented concentration were observed in high flow periods, and the sedimented concentration showed a slow increasing trend in the flood recession stage. High water velocity facilitated the microplastic particles to be migrated for a longer distance, and high water flow was conducive to transport more microplastics from source points. Besides, microplastic particles with high density had worse mobility in water and more prone to deposition. PET were likely to be transported for a relatively shorter distance, while PP had higher mobility and took less time to reach

\* Corresponding author.

E-mail address: [xlwang@apm.ac.cn](mailto:xlwang@apm.ac.cn) (X. Wang).

the same simulation point. This study put forward an effective approach to understand the transport of MPs in the river. The results obtained are useful to identify pollution hotspots and track pollution paths.

## 1. Introduction

Microplastic (MP) pollution is a global and pervasive environmental problem of growing concern owing to its ubiquity in the environment (Karbalaei et al., 2018; Bank and Hansson, 2022). MPs, defined as insoluble synthetic particles smaller than 5 mm, have been detected in different ecosystems, such as marine, lakes, rivers, aquaculture ponds, flood plain, groundwater, glacier, soil, and atmosphere (Petersen and Hubbart, 2021). Previous studies have shown that MPs widely exist in ecosystems, and their pollution concentration, distribution characteristics, and physical properties have also attracted the attention of many scholars (Niu et al., 2021; Du et al., 2021). In addition, relevant studies have confirmed that MPs are harmful to ecosystems, aquatic animals, and human health in the laboratory environment (Sana et al., 2020; De-la-Torre, 2020). Owing to their small size, high hydrophobicity, and relatively low density, MPs have ability to adsorb toxic substances in water, act as a potential carrier for microbial communities, accumulate in aquatic organisms, and transfer throughout the food web (Sharma and Chatterjee, 2017; Wang et al., 2020). MPs may infiltrate the body via the skin pores, digestive tract, and respiratory system, causing chemical and physical hazards to both animals and humans and inducing neurotoxicity and oxidative damage (Vethaak and Legler, 2021). The products from plastic degradation, such as phthalates, brominated flame retardants, bisphenol A, and bisphenone, may cause cancer (Blackburn and Green, 2021).

As the most indispensable and ubiquitous medium and carrier in nature, the river plays a key role in the transfer of MPs in the mainland (Kataoka et al., 2019). Freshwater systems are routinely more adjacent to terrestrial point sources and directly impacted by human activities (Windsor et al., 2019). Especially, river systems are sources of drinking water and food resources, and they harbor millions of people and aquatic organisms (Li et al., 2018). Although rivers and lakes are considered non-negligible sources for MPs entering the ocean, studies of MP pollution in freshwater systems fall far behind the marine counterpart (Du et al., 2020). Rivers are important channels in the transportation of land MPs, and they become the main source of marine MPs (Wang et al., 2021; Koutnik et al., 2021). Therefore, catchment-wide studies are critical to identify contamination hotspots and help understand associated ecological and human health risks (Hurley et al., 2018). The literature on freshwater MP contamination has increased rapidly in recent years (Talbot and Chang, 2022) owing to concerns about threats to aquatic ecosystems and risks to potable water supplies (Zhao et al., 2022). MPs in rivers are mainly from sewage treatment plants, agricultural pollution, industrial wastewater, cosmetic particles, and so on (Rochman, 2018). Owing to the high fluidity of water body and the influence of human activities, the process and mechanism of MP transport in rivers are very complex, the current research is insufficient.

In the river ecosystems, the transport and deposition behavior of MPs are significantly governed by hydrologic characteristics, storm events, hydraulic conditions, and their physical properties (Nizzetto et al., 2016; Eo et al., 2019). River hydrological characteristics, such as discharge, flow velocity, and water level, influence the suspension and deposition of MPs (Kumar et al., 2021). A recent study has indicated that rainfall is a source of MP contamination in freshwater systems and that rainfall not only helps MPs enter rivers and lakes but also carries MPs into the soil or wetlands (Xia et al., 2020). Studies have modeled the dispersion of traffic-related MPs from storm water to a river (Bondelind et al., 2020). Rainfall events have a significant impact on the MP budget in rivers (Hitchcock, 2020). Flooding events can potentially increase the transport and aggregation of MPs, and the abundance of MPs varies in different stages of a flood event (Chen et al., 2022). Besides, different

levels of flood events have different effects on the suspension, jumping, and settlement of different types of MPs (Eppehimer et al., 2021; Xu et al., 2022). However, compared with the study of MP pollution status in riverine ecosystems, the process and mechanism of MP transport in rivers remains sparse. The influence of rainfall events on the transport of river MPs is poorly investigated. Furthermore, at different stages of flood events, the transport characteristics and abundance differences of different types of MPs are unclear.

Considering the above knowledge gaps, this study proposed a hydrodynamic (HD) model coupled with the particle transport module on the basis of repeated field investigations and the characteristic parameters of the discovered MPs. The model was applied to analyze the MP transport in rivers. The specific objectives of the research are (1) to assess the spatiotemporal variation of composition and abundance between different types of MPs under different river hydrological regimes, (2) to investigate the influence of different rainfall events on the dispersal pattern, transport characteristics, and concentration difference, and (3) to examine the concentrations of different types of MPs at different stages of flood events. This study thus addresses two research gaps: (1) the limited investigation on the influence of different flow conditions on the dispersal and transport of MPs in the river and (2) the lack of knowledge in temporal and spatial differences of different types of MP abundance at various stages of rainfall events. The effects of rainfall events on the MP transport can be used to provide valuable information for MP source tracking and improve assessment of human and ecological health risks. Furthermore, this study emphasizes the effectiveness of comprehensive use of HD and particle tracking model to investigate the transport of MPs, which is of considerable importance for making decisions to better monitor and mitigate MP pollution.

## 2. Methodology

### 2.1. Case study area and data

The Hanjiang River, the longest tributary of the Yangtze River, is located between 106° and 114°E and 30–34°N. The basin is dominated by the sub-tropical monsoon, and the annual precipitation ranges from 700 mm to 1200 mm. The river is an important water supply to support agricultural, industrial, domestic, shipping, and ecological use. Meanwhile, Danjiangkou reservoir, located in the main stream, is the principal water resource provider for the South-to-North Water Diversion Project. The Danjiangkou Reservoir separated the Hanjiang River into upstream and middle-lower reaches. The section from Danjiangkou to Huangzhuang is the middle reaches. The upper reaches of the Hanjiang River mainly consist of woodlands with relatively undisturbed areas. In contrast, the middle and lower reaches is mostly occupied for residential, agricultural, and commercial activities, which receives various anthropogenically generated pollutants. Floodplains are densely distributed on both sides of the middle reaches of the river, and most of the banks of the lower reaches are artificially built embankments.

In this study, the specific modeling section is from Cihe Town and Gucheng County to Xiangyang City, located in the middle reaches of Hanjiang River (Fig. 1(a)). To better investigate the spatiotemporal variation characteristics of MP transport, one input source point (S1) and four monitoring points (M1-M4) are set up in the study river section. The monitoring points are distributed at a relatively uniform distance, and they reflect changes in land use. The vicinity of monitoring point 1 (M1) is mainly agricultural land, and the two banks of monitoring point 2 (M2) are large floodplains. The south bank and north bank of monitoring point 3 (M3) have a large number of farmlands and industrial parks, respectively. Monitoring point 4 (M4) is located in the main urban

section, and the north bank is an urban park. The discharge and water level data were obtained from the Hubei Province Hydrology and Water Resources Bureau, and the cross-sectional topographic data were obtained from the China Yangtze River Water Resources Commission. The meteorological data were obtained from the China Meteorological Data Sharing Network.

## 2.2. Model development

### 2.2.1. Hydrodynamic model

In this study, we coupled the particle tracking module with the flow module to study the MPs transport in rivers. The Hydrodynamic module is the basic computational component of the MIKE 21 Flow Model modeling system, and it provides the HD basis for the particle tracking module (DHI, 2017). The HD module is based on the depth-integrated incompressible Reynolds-averaged Navier–Stokes equations (Lu et al., 2020). The topography of the study area was defined using a flexible unstructured grids. Flow and water level variations are described by the Saint-Venant equations, which were expressed as follows:

$$\frac{\partial h}{\partial t} + \frac{\partial p}{\partial x} + \frac{\partial q}{\partial y} = w \quad (1)$$

$$\begin{aligned} \frac{\partial p}{\partial t} + \frac{\partial}{\partial x}\left(\frac{p^2}{h}\right) + \frac{\partial}{\partial y}\left(\frac{pq}{h}\right) + gh\frac{\partial z}{\partial x} + gp\frac{\sqrt{p^2 + q^2}}{c^2 h^2} \\ - \frac{1}{pw}\left[\frac{\partial}{\partial x}(ht_{xx}) + \frac{\partial}{\partial y}(ht_{xy})\right] + \frac{h}{pw}\left(\frac{\partial p_a}{\partial x}\right) \\ = 0 \end{aligned} \quad (2)$$

$$\begin{aligned} \frac{\partial q}{\partial t} + \frac{\partial}{\partial y}\left(\frac{q^2}{h}\right) + \frac{\partial}{\partial x}\left(\frac{pq}{h}\right) + gh\frac{\partial z}{\partial y} + gq\frac{\sqrt{p^2 + q^2}}{c^2 h^2} \\ - \frac{1}{pw}\left[\frac{\partial}{\partial y}(ht_{yy}) + \frac{\partial}{\partial x}(ht_{xy})\right] + \frac{h}{pw}\left(\frac{\partial p_a}{\partial y}\right) \\ = 0 \end{aligned} \quad (3)$$

where  $h$  is the water depth (m);  $w$  is the net incoming flow rate (m/s);  $z$  is the surface elevation (m);  $(p, q) = (hu, hv)$  are the flux densities in directions  $x$  and  $y$ , respectively ( $\text{m}^2/\text{s}$ );  $C$  is the Chezy resistance ( $\text{m}^{1/2}/\text{s}$ );

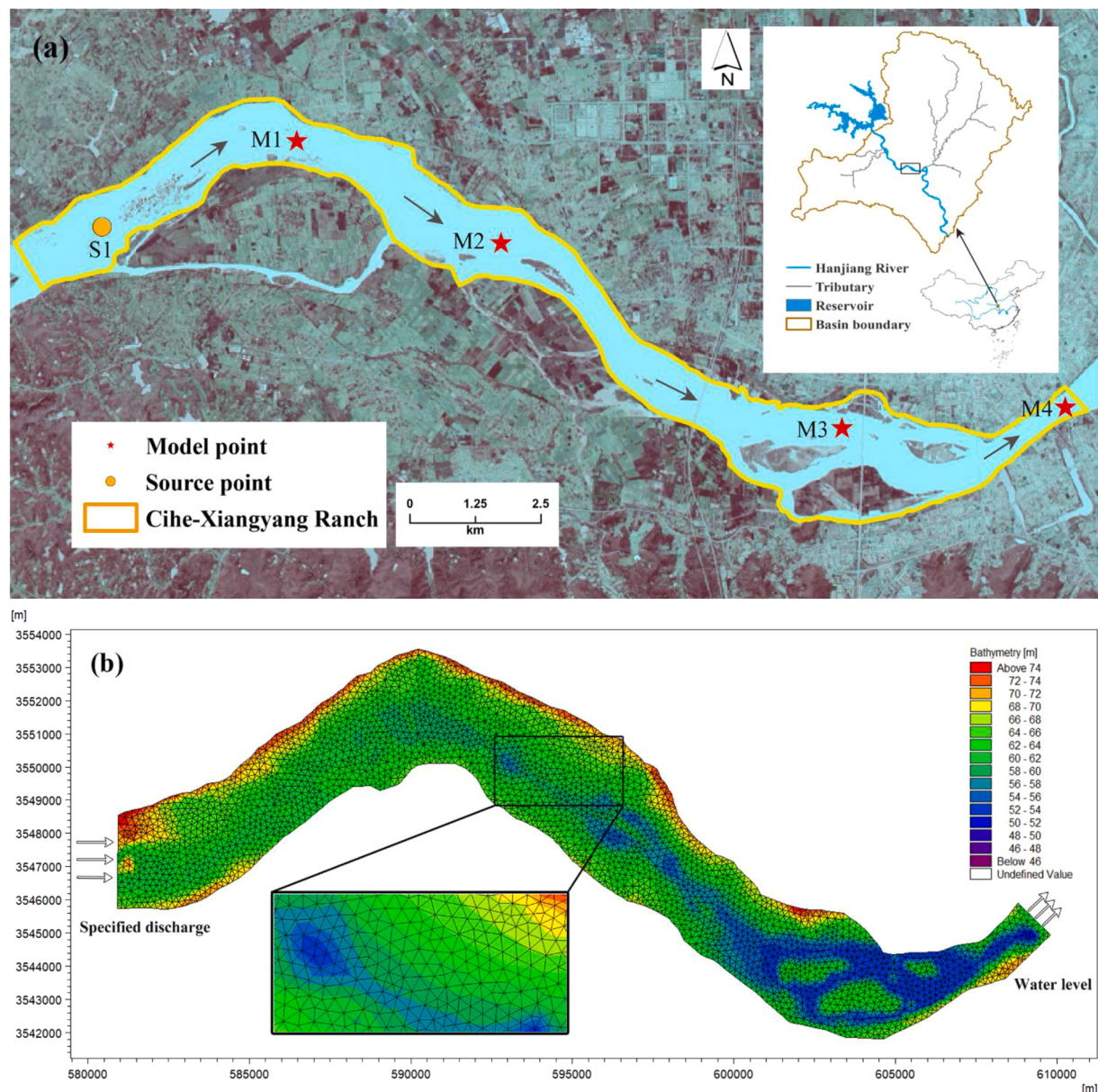


**Fig. 1.** The study site with selected source and monitoring points (a) and the bathymetry files (b).

$g$  is the gravitational gravity ( $\text{m/s}^2$ );  $p_w$  is the density of water ( $\text{kg/m}^3$ );  $p_a$  is the atmospheric pressure ( $\text{kg/m/s}^2$ ); and  $\tau_{xx}$ ,  $\tau_{yy}$ , and  $\tau_{xy}$  are the components of effective shear stress.

### 2.2.2. Particle tracking module

In this study, the particle tracking module of MIKE 21 Flow Model is applied to simulate the transport process and determine the fate of suspended and sedimented microplastic particles. In this module, the transport and dispersion process of particles were described by the Langevin equation (DHI, 2017). The motion of each microplastic particle and the change in concentration are recorded and described as functions of time independently of reference mesh system depending on the HD input. And the model results were depicted and analyzed with a spatial analysis approach. The resulting equations are expressed as follows:

$$dX_t = a(t, X_t)d_t + b(t, X_t)\xi_t d_t \quad (4)$$

where  $a$  and  $b$  are the drift term and diffusion term, respectively,  $\xi$  is the random number. The Euler estimation  $Y$  for a given time from the initial value of  $Y_0 = X_0$  was discretized to simulate a trajectory, which then yielded the following equations:

$$Y_{n+1} = Y_n + a(t, X_t)Y_n\Delta_n + b(t, X_t)Y_n\Delta W_n \quad (5)$$

$$\Delta W_n = W_t - W_s \in N(\mu = 0, \sigma^2 = \Delta_n) \quad (6)$$

where  $n = 1, 2, 3, \dots$ , according to the Euler scheme with drift  $a$  and diffusion coefficient  $b$ . And  $\Delta W_n$  is the normal distributed Gaussian increment of the Wiener process  $W$ , which is a continuous-time Gaussian stochastic process with independent increments over the subinterval  $\tau_n \leq t \leq \tau_{n+1}$ .

After each time step the parcels are summarized in each cell of the grid system, a derived concentration field is calculated using the following equation:

$$C_k = \frac{\sum_{i=1}^{N_k} M_i}{V_k} \quad (7)$$

where  $k$  is the ID number of cell in reference grid system;  $C_k$  is the concentration in cell  $k$  of the reference grid system;  $M_i$  is the mass of particle  $i$ ;  $N_k$  is the number of particles within cell  $k$ . The concentration field, particles with positions and masses can be derived in the particle list output from the Particle Tracking Module.

### 2.3. Mesh grid establishment and boundary condition setting

In the HD module, the mesh file was created in the MIKE Zero Mesh Generator, coupled water depths with different geographical positions, and included the computational grid, node connectivity, and boundary information. Setting up the mesh included setting adequate bathymetry and defining codes for open and closed boundaries. The latest Landsat-8 satellite images were used to help delineate river boundaries. The topographic data file (xyz.) was extracted in ArcMap based on the measured 205 cross-section topographic and DEM data with the spatial resolution of 30 m.

In this study, two open boundary conditions were defined from the mesh file specified in the domain parameters: a north boundary (code 4) and a south boundary (code 3). One was for the upstream boundary conditions consisting of daily discharge time-series at Gucheng station (code 4). The another was for the downstream boundary conditions consisting of daily water level time-series at Yujiahu station (code 3). The computational grid and bathymetry files are shown in Fig. 1(b).

### 2.4. Model parameter setting and calibration

The horizontal eddy viscosity type was chosen to a flux based on

Smagorinsky formulation, and a constant Smagorinsky coefficient was specified with a value of 0.285. The minimum ( $1.8 e^{-0.006} \text{ m}^2/\text{s}^2$ ) and maximum ( $\max 10^7 \text{ m}^2/\text{s}^2$ ) values of eddy viscosity were specified. The length of warm-up period was set to 720 s. Initial condition of surface level was set up with a value of 0.0 m. The effects of the wind speed and wind direction on the flow field were taken into account in this study. A constant wind friction coefficient of 0.001932 was applied. The format of the wind data varied in time and constant in domain based on the meteorological data of the nearest meteorological station. Manning's ( $n$ ) resistance formula was applied and optimized in this study during the model calibration. The values of 0.0339, 0.0527, 0.0318, and 0.0226 were finally specified for the Cihe Town to Loupo Village, Loupo Village to Niushou Town, Niushou Town to Huyang Village, and Huyang Village to Hanjiang Changhong Bridge reaches of the river, respectively.

On the basis of the field samples collected from 19 sampling sites along the middle and lower reaches of Hanjiang River before the simulation, polyamide (PA), polyethylene (PE), polypropylene (PP), polystyrene (PS), and polyethylene terephthalate (PET) were identified as the dominant MP types in the study catchment (Junaid et al., 2022; Dong et al., 2022). Their common usage on a daily basis was also considered. Particles were divided into five different classes (PA, PE, PP, PS, and PET) in this simulation. Each class has specific properties regarding, settling/buoyancy, erosion, and dispersion that must be specified separately. Source location is fixed at position (Easting 581257, Northing 3546473). All five MPs classes were released from source point at a rate of 1 g/s, and ten particles were released per time step. A maximum particle age of 7200 s was specified. The settling velocities of the simulated MPs of different particle sizes were obtained from the laboratory experimental study (Waldschläger and Schuttrumpf, 2019). The most commonly identified densities across a range of studies were used as the baseline density value for each modeled MP type (Kumar et al., 2021). The density of PA, PE, PP, PS, and PET were identified at approximately  $1.15 \text{ g/cm}^3$ ,  $0.93 \text{ g/cm}^3$ ,  $0.89 \text{ g/cm}^3$ ,  $1.08 \text{ g/cm}^3$ , and  $1.37 \text{ g/cm}^3$ , respectively. The horizontal and vertical dispersion were set using a dispersion coefficient formulation with a constant value of  $5 \text{ m}^2/\text{s}$ . The drift profile was defined by the surface wind acceleration with a wind weight of 0.1, a wind drift angle of 28, and a kinematic viscosity of  $1.14 \times 10^{-6}$ . The bed roughness and wind forcing were taken from the HD model. Decay and erosion were excluded for the five classes. The optimal time step was 60 s after trying different time steps higher than 1 s

The MIKE 21 Flow Model was calibrated and validated using daily discharge data. Two base flow time periods and six flood events with different recurrence intervals were used for calibration and validation. The base flow periods were selected based on the local climate characteristics and the long term hydrological observation data, the middle and lower reaches of the Hanjiang river are divided into three hydrological periods: wet period (June to September), dry period (December–February) and normal water period (March to May and October to November). Two basic flow time series were selected in the normal period from March 1 to April 12, 2021 and April 12 to April 29, 2022. In these two periods, we conducted hydrological field investigation in the middle and lower reaches of the Hanjiang River, and monitored the flow, water level and bottom topography of the studied river section, which complemented the hydrological data obtained from the hydrological station, and played an important role in the model construction and parameter calibration process. The calibration and validation fits were statistically evaluated using several indicators. Nash–Sutcliffe efficiency (NSE), ratio of the root mean square error to the root mean square error (RMSE), and percent bias (PBIAS) were calculated to estimate errors between the simulated and the measured values (Moriasi et al., 2015; Noori and Kalin, 2016).

### 3. Results

#### 3.1. Performance evaluation of the model

The performance of the model was evaluated using the NSEC, PBIAS, and RMSE of the measured data. Table 1 shows the evaluation of the MIKE 21 Flow Model results in the calibration and validation phases. In the calibration phase, NSEC values of 0.91, 0.93, and 0.94 were observed under 50-year flood, 20-year flood, and 10-year flood event, respectively. NSEC value of 0.96 was obtained during base flow period. PBIAS values of -1.21, 1.07, -0.41, and 0.87 were observed under base flow scenario, 50-year flood, 20-year flood, and 10-year flood event, respectively. The best RMSE value was obtained during base flow period. In the validation phase, NSEC values of 0.92, 0.87, and 0.92 were observed under 50-year flood, 20-year flood, and 10-year flood event, respectively. PBIAS values of 1.13, 0.76, and 0.32 were observed under 50-year flood, 20-year flood, and 10-year flood event, respectively. The RMSE value during the base flow simulation period is significantly better than that of the three flood periods. Furthermore, a scatter plot of the observed and simulated values of the discharge time series is shown in Fig. 2 to compare the calibration and validation model results. The amounts of high and low discharge were modeled effectively under one base flow and three different levels of flood events. The results were satisfactory on the basis of the performance rating of model evaluation criteria recommended by Moriasi et al. (2015), and the model was suitable for tracking the features of observed hydrologic characteristics.

#### 3.2. Concentration of different types of MPs under flood event scenarios with different recurrence intervals

The distribution characteristics of total suspension concentration under different simulation scenarios are shown in Fig. 3(a). The concentration data distribution was the most dispersed and concentrated under the 10-year and base flow scenario, respectively. With the increase of flood intensity, the mean value, maximum value and minimum value of suspended concentration all increased. The distribution characteristics of total sedimented concentration under different simulation scenarios are shown in Fig. 3(b). Compared with the total suspended concentration, the total sedimented concentration distribution under the base flow scenario, 20-year scenario and 50-year scenario was more concentrated, while the sedimented concentration distribution data under the 10-year scenario was more scattered. The mean and median of the sedimented concentration were significantly higher under the 10-year scenario than those in other scenarios. The results for suspended concentration of different types of MPs under different discharge scenarios are shown in Fig. 4. In the simulation of base flow scenario, with the increase of discharge value, the total suspended concentration of the five kinds of MPs showed a significant increasing trend. From the perspective of individual MP types, the suspension concentration of PA and PP particles showed an increasing trend with the increase of discharge. By contrast, the effect of discharge change on the suspension concentration of PS and PET was not significant. The suspension concentration of PET particles under the three flood events simulation scenarios was significantly higher than that under the base flow condition. Besides, in the flood rising stage, the suspension concentration of

MPs increased rapidly but decreased relatively slowly in the flood recession stage. In addition, when the discharge reached the peak, the MP concentration did not obtain the maximum at the same time, but within one to three days after the peak discharge. This implied a significant lag effect between the concentration of MPs and peak flow.

The sedimented concentration of MP particles in different levels of flood event scenarios greatly varied from the suspended concentration (Fig. 5). In the base flow simulation scenario, the relationship between the total sedimented concentration of MPs and the discharge was not significant. The concentration of PE particles was significantly higher than that of other types of particles. However, in the flood events with 10-year recurrence interval scenario, the sedimented concentration of MPs showed a trend of first decreasing and then slightly increasing, and reached the minimum value five days after the peak flow appeared. In the flood events with 50-year recurrence interval scenario, the sedimented concentration of MP particles was significantly lower than that in the 20-year flood events. In the flood rising stage, the concentration of sedimented particles was relatively stable. Upon entering the high flow stage, the sedimented concentration of MP particles showed a downward trend and reached the minimum value after the peak flow appeared. In the flood recession stage, the sedimented concentration showed a slow increasing trend. The sedimented MP particles in the riverbed were easy to be moved again in the high flow stage, and resuspension occurred. After the MP concentration reached the maximum, the discharge peak reached the maximum within 1–3 days, and after the discharge peak, the MP deposition concentration fluctuated greatly, which indicated that the difference of MP concentration caused by different rainfall types is different.

Similar to the results of this research, some recent studies also indicated that flood events have a significant impact on the microplastic concentration in rivers (Cheung et al., 2019), the 10 year return period floods increased tenfold the global plastic mobilization potential in the worst affected regions compared to non-flood conditions (Hitchcock, 2020). Weideman et al. (2019) observed low MPs abundance in the pre-flooding events but large abundance after flooding at the downstream side, but did not distinguish between deposition and suspension concentrations. Additionally, a close relationship between microplastic abundance of surface water in Donghu Lake and flood events was identified, the microplastic abundance was significantly affected by rainfall (Xia et al., 2020). Nevertheless, studies to identify the impact of flood events on the transport of microplastics in rivers is still sparse. And influence mechanism should be investigated case by case, as the meteorological characteristics, topographic features and the hydrological situation of the study area will vary among different areas.

#### 3.3. Differences in dispersal and transport among MP types

The daily travel distances of MP particles in four flood event scenarios with different recurrence intervals are shown in Fig. 6. In the base flow, 10-year, and 20-year simulation scenario, the five kinds of MP particles all moved in the opposite direction on some dates. With the increase of flood level, the number of days of reverse movement gradually decreased. Under the 50-year flood event scenario, the phenomenon of reverse movement was not observed. The variation rate of the daily movement distance of MP particles decreased significantly in the 20-year and 50-year flood events scenario. Compared with the simulation results of base flow scenario, the daily moving distance of MP particles in 20-year and 50-year flood events has increased slightly. Additionally, in the 50-year flood event simulation scenario, the particle transport distance showed preliminary consistency with the discharge change, and this change characteristic was not significant in the basic flow and the 10-year simulation scenario.

To better identify the distance and time characteristics of different types of MP particles, we selected four monitoring points in the study area for comparative analysis. The migration distance and age characteristics of MP particles in four flood events scenarios with different

**Table 1**  
Evaluation of the MIKE 21 FM model results of discharge under different rainfall events.

Statistical criteria	Calibration			Validation		
	NSEC	RMSE	PBIAS	NSEC	RMSE	PBIAS
50 yr flood	0.91	736.56	-1.21	0.92	300.14	1.13
20 yr flood	0.93	815.72	1.07	0.87	130.10	0.76
10 yr flood	0.94	314.44	-0.41	0.92	390.54	0.32
Base flow	0.96	67.50	0.87	0.91	13.77	0.14

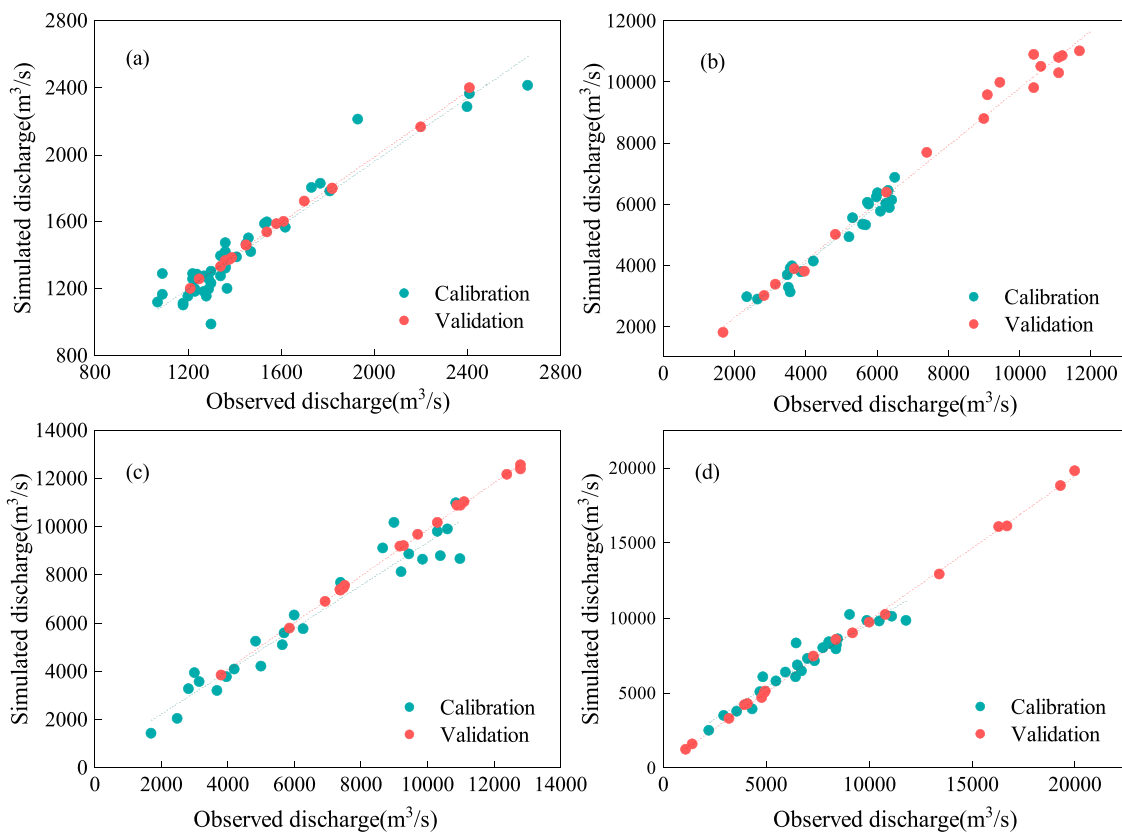


**Fig. 2.** Scatter plot between observed and simulated values in the calibration and validation phases. Base flow: (a); 10 <sup>yr</sup> flood flow: (b); 20 <sup>yr</sup> flood flow: (c); 50 <sup>yr</sup> flood flow: (d).

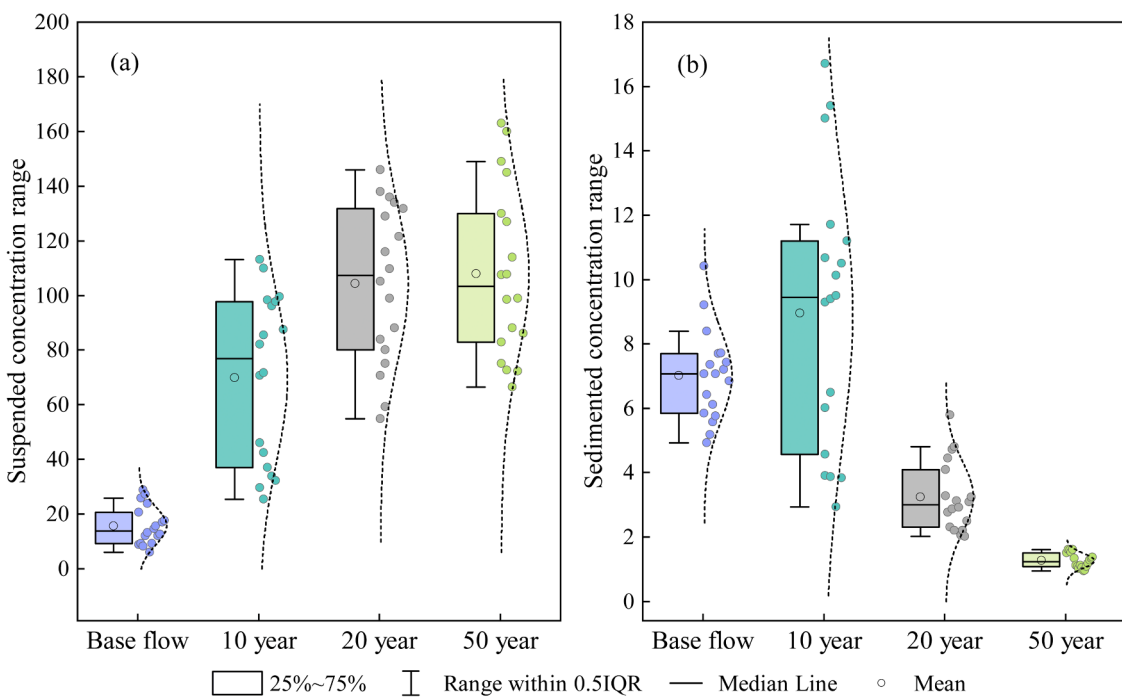


**Fig. 3.** Data distribution box diagram of total concentration of microplastics. Suspended concentration: (a); Sedimented concentration: (b).

recurrence intervals were shown in Fig. 7. In M1 point, the longest and the shortest transport distance was obtained under the base flow (PS particles) and 10-year flood events scenario (PET particles) respectively. The migration distance of PS particles in the base flow and 50-year flood

events scenario was higher than that in other types of particle. Compared with the results under base flow scenario and 50-year flood events, it took longer for PE, PA, PS, and PET particles to reach M1 in 10-year and 20-year flood events, and among the five types of microplastics,

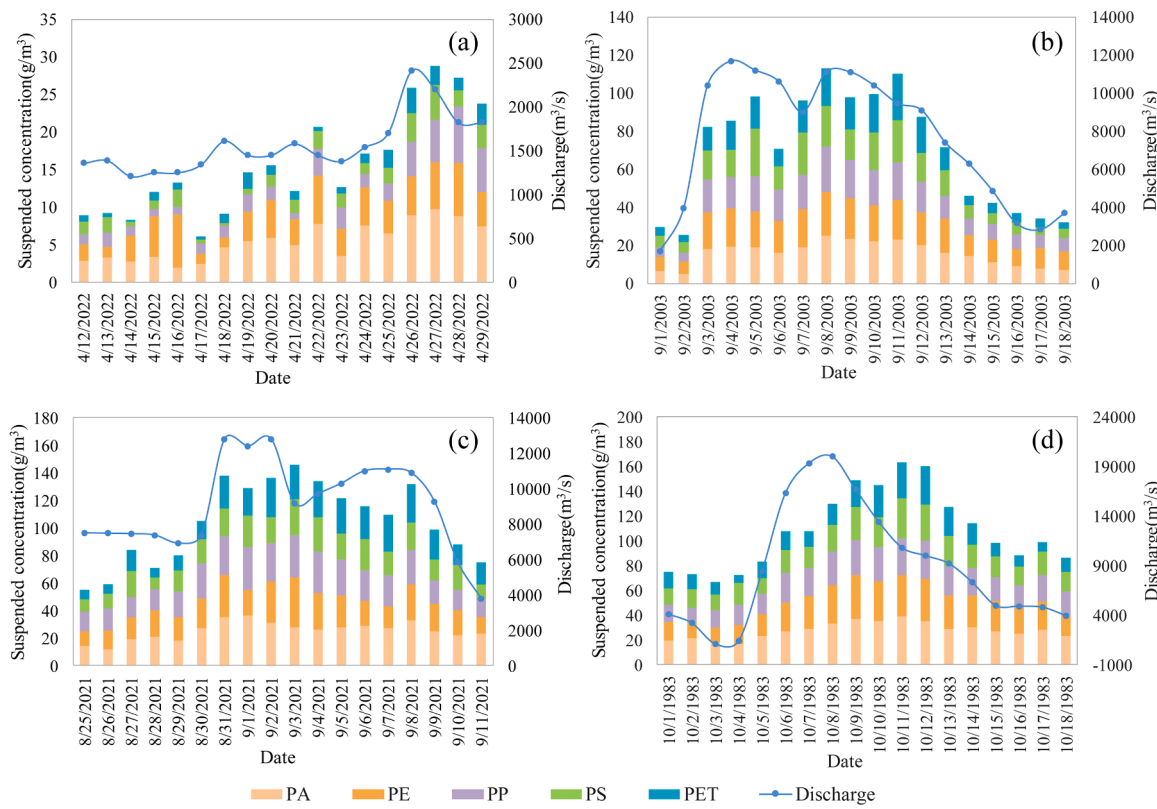


**Fig. 4.** Suspended concentration of different types of MPs under different flood events scenarios with different recurrence intervals. Base flow: (a); 10<sup>yr</sup> flood flow: (b); 20<sup>yr</sup> flood flow: (c); 50<sup>yr</sup> flood flow: (d).

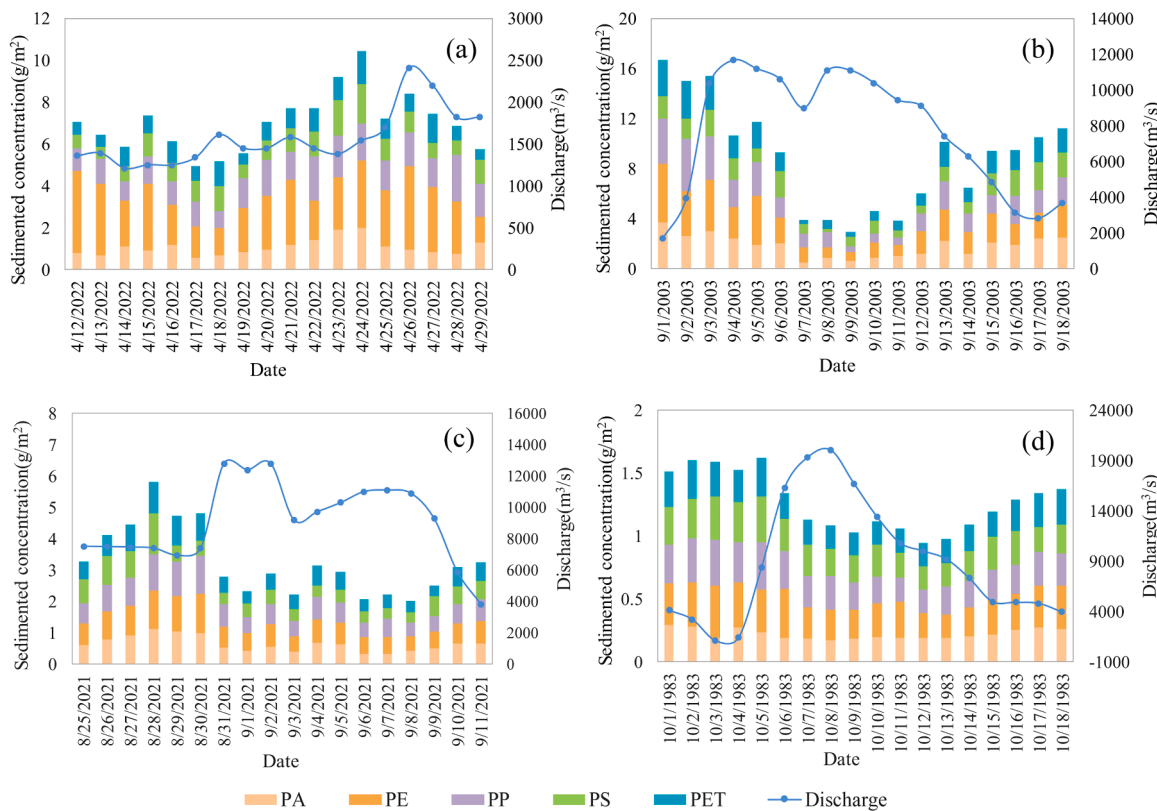


**Fig. 5.** Sedimented concentration of different types of MPs under different flood events scenarios with different recurrence intervals. Base flow: (a); 10<sup>yr</sup> flood flow: (b); 20<sup>yr</sup> flood flow: (c); 50<sup>yr</sup> flood flow: (d).

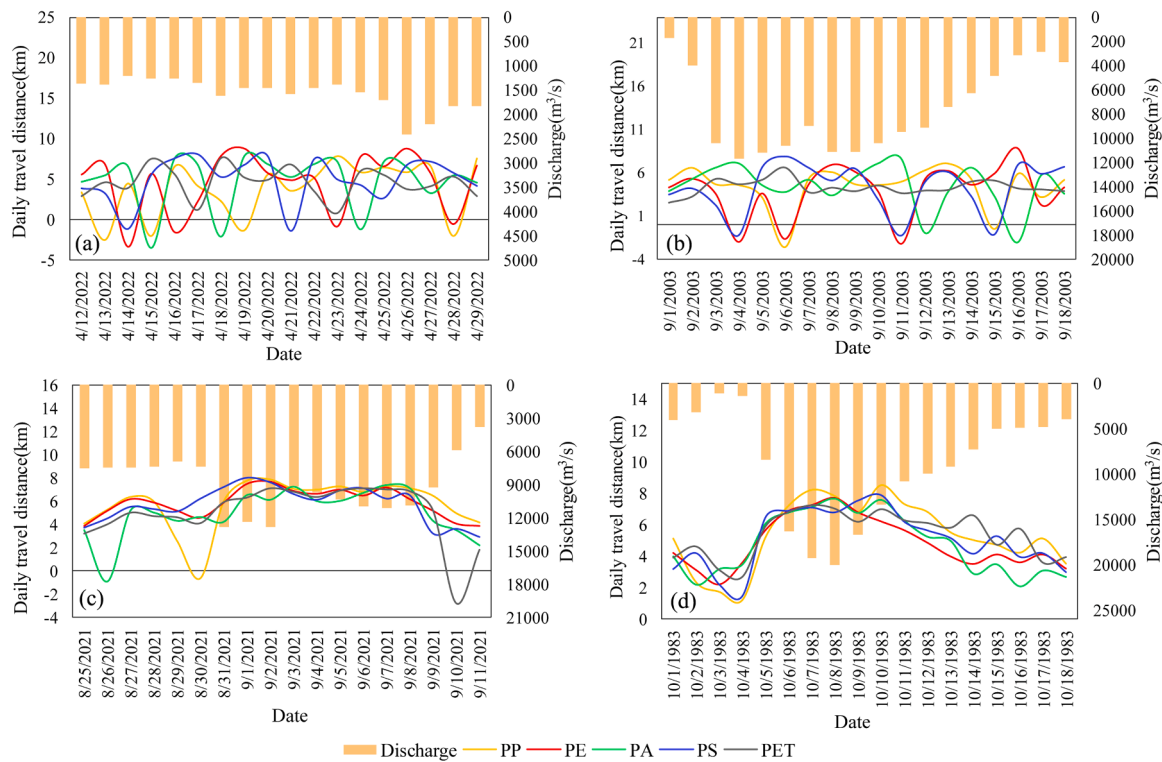


**Fig. 6.** Daily travel distance of different MP particles under four flood events scenario with different recurrence intervals. Base flow: (a); 10 <sup>yr</sup> flood flow: (b); 20 <sup>yr</sup> flood flow: (c); 50 <sup>yr</sup> flood flow: (d).

PET took the longest time to reach point M1 in four simulation scenarios. In M2 point, MP particles migrated the longest and shortest distances under 50-year flood events and base flow scenario. Similar to M1 point, PET was observed to be the particle types with the longest migration age. Simulation results indicated that flood magnitude has significant effect on the transportation process of MP particles. Besides, the data extracted at M1, M2, and M4 all showed that the migration time of PP particles were significantly smaller than that of PET. PP is one of the lightest polymers among all commodity plastics, the average density of PP is 0.89 g/cm<sup>3</sup>. And yet the average density of PET is 1.37 g/cm<sup>3</sup>, which is significantly higher than that of PP. Since biological and physical degradation processes are not considered in the particle transport model, density and weight are the main factors that cause the differences in transport distance and age of different types of microplastics. The results showed that the microplastic particles with low density move faster than those with high density. To-date, only a few studies have investigated the transport of different types of microplastic in aquatic ecosystem. Similarly, recent studies have shown the differences between the transport processes of different types of microplastics, the dispersal processes of PE, PP, PA, and PET microplastic particles in river sediments were investigated, and the results confirmed that microplastics with lower density would have higher mobility in river sediments. PP and PE are likely to be migrated for a longer distance, at the same time, PET and PA tended to accumulate near to source points (He et al., 2021).

#### 3.4. Influence of discharge and velocity changes on suspension concentration of MPs

To further reveal the impact of key hydrological factors on the transport of MPs, the relationship between flow velocity and MP suspension concentration under different flood events was fitted and analyzed. Multiple fitting function expressed the relationship between flow velocity and suspension concentration of MPs (Fig. 8). In the base flow scenario, the suspension concentration of MPs showed an

increasing trend with the increase of flow velocity, and  $R^2$  value of 0.6682 was obtained in the fitting regression. Compared with the base flow scenario, the relationship between suspension concentration and flow velocity in the flood events with 10-year and 20-year recurrence interval scenario were better fitted, and  $R^2$  values of 0.7223 and 0.7209 were obtained, respectively. In the flood events with 50-year recurrence interval scenario,  $R^2$  value of 0.6754 was obtained in the fitting relationship, and the distribution characteristics of scattered points suggested that the low velocity stage had a better correlation than the high velocity stage. This implied that the rising phase of flow velocity was often accompanied by the increase of MP concentration.

The relationship between discharge and MP suspension concentration under different flood events was fitted (Fig. 9). In the base flow scenario, the suspension concentration of MPs showed a significant increasing trend with the increase of discharge, and  $R^2$  value of 0.6679 was obtained in the fitting regression. In the flood events with 10-year and 20-year recurrence interval scenario, there was a similar relationship between the MP suspension concentration and discharge, and  $R^2$  values of 0.86 and 0.772 were obtained in the fitting regression respectively. In the 50-year flood events scenario, the change relationship between discharge and suspended concentration was different from other simulation scenarios, the high suspension concentration value was not maintained in the high flow stage. Previous relevant studies showed that high river flow would transport more microplastics from source points, and high flow velocity in bottom water layer are identified to be conducive to the transport of microplastics in river sediments, conversely, slow velocity was more favorable for shorter transport distances and MP particles deposition (He et al., 2021), which was similar to the results in the base flow, 10-year, and 20-year flood events simulation of this study, but the transport concentration under the extreme flood events scenario has not been identified. Besides, interactions between flow magnitude and MPs concentrations in the aquatic ecosystem were also discussed by Wu et al. (2020) and Chen et al. (2021). Based on their results, larger MPs with densities marginally higher than water can retain in the sediment. High flow periods can remobilize the

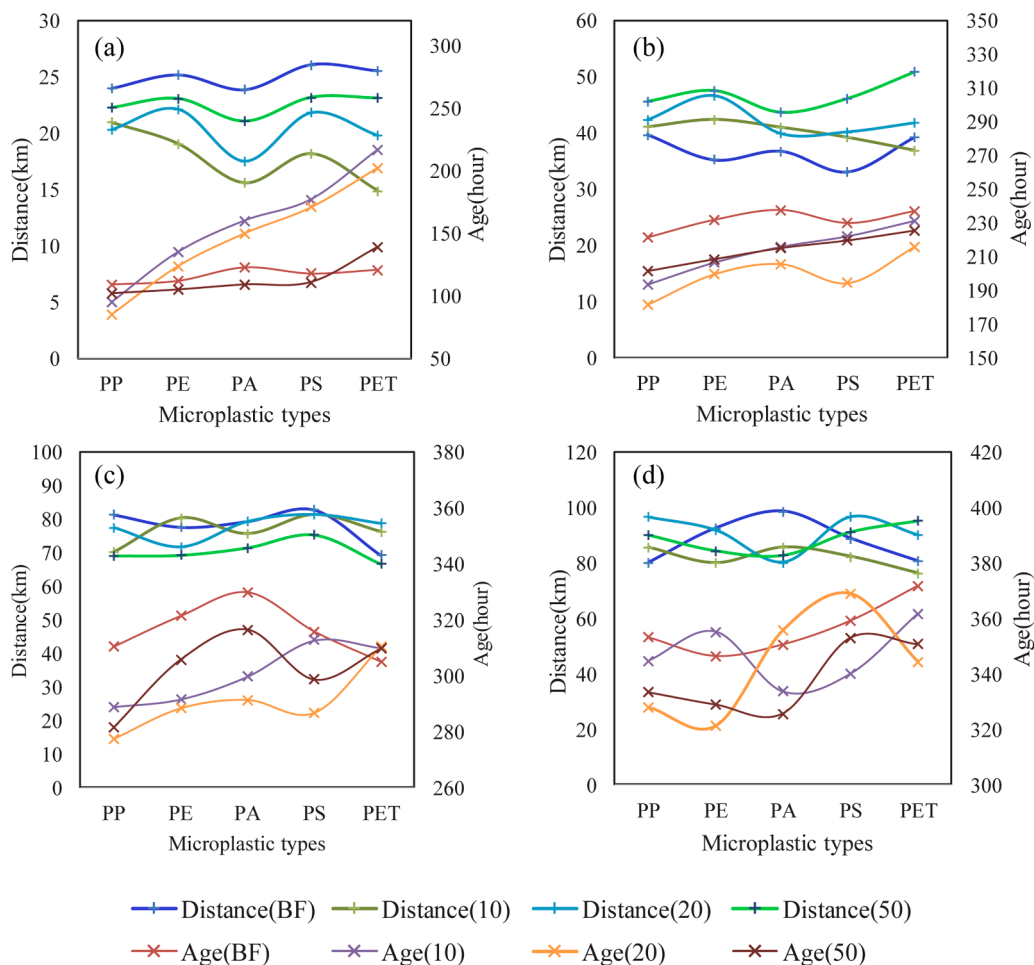


Fig. 7. Transport distance and age of the MPs particles at different monitoring points. M1: (a); M2: (b); M3: (c); M4: (d).

microplastic particles deposited before, thus river sections with relatively slow velocity was more likely to be the hotspot of microplastics accumulation (Nizzetto, 2016).

#### 4. Discussions

This study identified the concentration difference of different MPs under flood event scenarios with different recurrence intervals, and quantified the relationship between river flow, velocity, and MP suspension concentration. There was a significant positive correlation between the total suspension concentration of microplastic particles and the flow velocity. But, the synergistic increase of discharge and suspended concentration was only observed in the base flow, 10-year and 20-year flood events scenarios. In the 50-year flood event scenario, the synergistic increase of suspended concentration and discharge was not well maintained in the high flow period. This phenomenon was not observed in the synergistic relationship between flow velocity and suspension concentration. With an increased discharge, the ability to transport microplastics particles also be enhanced. However, since the microplastics release position and release rate set in the simulation were fixed, the increase of microplastics concentration was limited by the release amount at the source point. The change of flow velocity is not only related to the discharge, but also affected by the topographic height difference of the river bed. Therefore, the relationship between flow velocity and microplastics concentration was different from that between discharge and concentration. Furthermore, the suspension concentration and sediment concentration of different MP particles were based on continuous release at fixed location. In actual rivers, the

sources of MPs are diverse and may move into the flow from anywhere along the river. Furthermore, owing to complexity and uncertainty of the MPs' fragmentation properties and biological effects, degradation was not addressed in the simulation. The shape and density of MP particles can change, with residence time in the riverine ecosystem due to aggregation, biofilm development, degradation, and flocculation mechanisms.

This study provided an effective approach to understand the dispersal and movement of different MPs in the river. On the basis of the river's HD process, the differences in suspension concentration and sediment concentration of MPs in base flow and different flood events were identified. The modeling results confirmed that MP particles not only floated in water and were transported by water flows but also detained and accumulated in the river bed. River hydrological characteristics, such as bed forms, flow velocity, and discharge, influence the MP concentration. Similarly, riverbed or riparian vegetation may retain MP particles and allow MP deposition when water velocity is declining. However, owing to the spatiotemporal heterogeneity of influencing factors of MP transport, various factors underpin the lack of consistency in their observations. In particular, parameters related to aquatic organisms are difficult to quantify and evaluate. In this simulation, the influence of river bottom vegetation on MP transport was not considered. Besides, the results emphasize the importance of river hydrological regimes as controls on the transport of MP particles, which parallels the situation with river sediments. The complex relationships between river flows and sediment concentration reflect the dynamic process of fine material within river channels, such as suspension, resuspension, and settlement. Furthermore, there are differences in the migration of MPs in

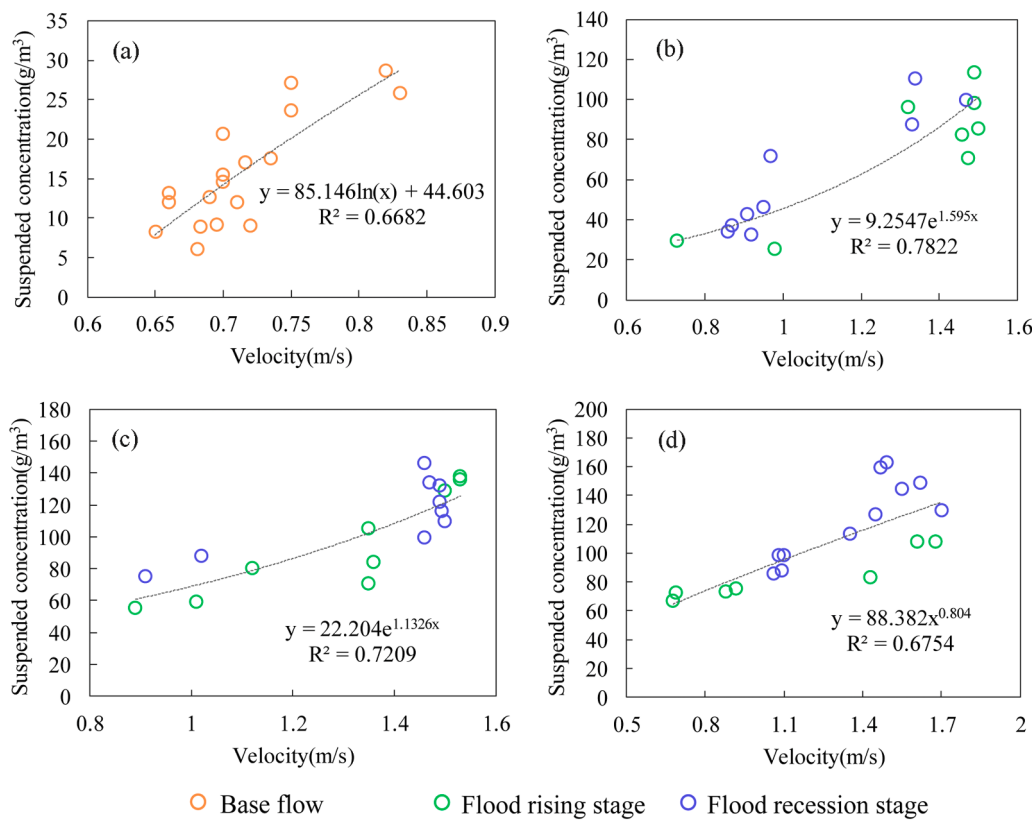


**Fig. 8.** Relationship between flow velocity and suspension concentration of MPs. Base flow: (a); 10 <sup>yr</sup> flood flow: (b); 20 <sup>yr</sup> flood flow: (c); 50 <sup>yr</sup> flood flow: (d).

water environments with different sediment concentrations owing to the interaction between MPs and sediment particles. Therefore, further studies are recommended to consider the cooperative migration of sediment particles during MP transport.

The results showed the concentration difference of MP particles under four flood event scenarios with different recurrence intervals. The types of MPs showed certain variations under different discharge scenarios. In the flood rising stage, the suspension concentration of MPs increased rapidly but decreased relatively slowly in the flood recession stage. The time lag between discharge and MP concentration were observed in the four simulation scenarios. Besides, the distance and age characteristics of different types of MP particles were identified in the four simulation scenarios, results showed that there was no significant consistency between the distance and age of particle migration. The lag in the response to the river discharge peak and inconsistency between distance and time may suggest that the influence of river bottom topography on the suspension, transport, resuspension, and sedimentation of MP particles cannot be ignored. Heterogeneity of topographic conditions in different river sections may also be one of the influencing factors, which needs to be quantified in further research. Furthermore, PP particles showed the strongest transport capacity in the four different simulation scenarios, whereas PET showed the worst transport capacity. The migration distance and age characteristics of different MP particles in the simulation results implied that flood process has significant effect on the migration of MP particles. Especially under extreme flood events, low density MPs can travel for longer distance. Therefore, in the investigation of MP pollution in rivers, the abundance before and after the flood event should be compared, and the difference investigation should be carried out at various stages of the flood. This study provided an effective tool that can help in the design of optimum sampling points and frequencies.

## 5. Conclusion

This study proposed an effective approach to understand the dispersal and transport of different MPs in the river. The migration distance and age characteristics of MP particles were calculated through a velocity field in the hydrodynamic model coupled with the particle tracking module. Concentration of different types of MPs under flood event scenarios with different recurrence intervals were identified. And the influence of discharge and velocity changes on suspension concentration of MPs were investigated. Results showed that rainfall intensity had a significant impact on the microplastic concentration in rivers, high flow was accompanied by low deposition concentration and high suspension concentration. Density has a significant effect on the movement rate of microplastic particles, microplastic particles with lower density had stronger mobility in river flow. Under the same flow conditions, the migration rate of PET particles was lower than that of PP. PP particles were likely to be transported for a relatively longer distance and took less time to reach the same simulation point.

This study well demonstrated the spatiotemporal differences of MPs' transport characteristics under different hydrological conditions. It emphasized the importance of river hydrological regimes on the migration and deposition of MPs. The simulation results under different rainfall event scenarios suggested that rainfall has a strong ability to transport MP particles in the river environment. MP particles are not only transported but also settled down to the river bed. The marked temporal variation of concentrations in flood events imply the need for repeat surveys, especially to include samples at different discharge conditions. Particle tracking simulation is expected to provide important information for source tracking with the pollution of different MP types. Considering the similar complex relationship between river sediment and hydrological regime, further studies are therefore recommended to consider the synergistic transport mechanism of sediment and MP particles.

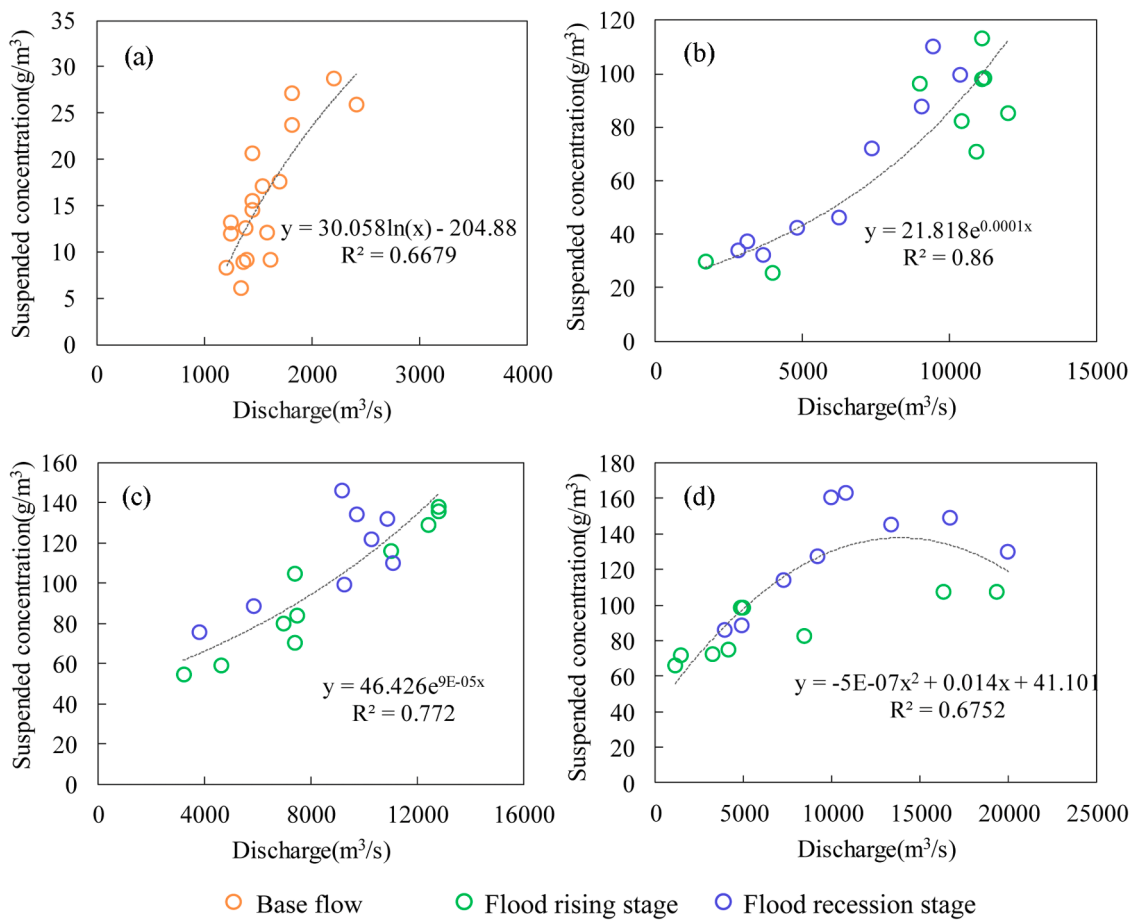


**Fig. 9.** Relationship between discharge and suspension concentration of MPs. Base flow: (a); 10 yr flood flow: (b); 20 yr flood flow: (c); 50 yr flood flow: (d).

## **Environmental implication**

Previous studies have confirmed that microplastics are harmful to ecosystems, aquatic animals, and human health. Microplastics have ability to adsorb toxic substances in water, act as a potential carrier for microbial communities, accumulate in aquatic organisms, and transfer throughout the food web. River plays a key role in the transfer of microplastics in the mainland. This study provided valuable information for microplastics source tracking and improved assessment of human and ecological health risks. Results emphasized the effectiveness of HD and particle tracking model to investigate the transport of microplastics, which is of great significance to monitor and mitigate microplastics pollution.

## CRediT authorship contribution statement

Xiaorong Lu proposed the idea and designed the study; Xiaorong Lu and Xuelei Wang analyzed the results and prepared the manuscript; Xi Liu made substantial contributions to interpretation of the data; Vijay P. Singh polished language of the manuscript.

## **Declaration of Competing Interest**

The authors declare that they have no known competing financial interests or personal relationships that could have appeared to influence the work reported in this paper.

## Data Availability

Data will be made available on request.

## Acknowledgments

This work was supported by the Postdoctoral Research Foundation of China (No. 2020M682526); the National Natural Science Foundation of China (No. 42207533, 41571202); the Nature Science Foundation of Hubei Province (No. 2021CFB187).

## References

- Bank, M.S., Hansson, S.V., 2022. The microplastic cycle: an introduction to a complex issue. *Microplastic in the Environment: Pattern and Process*. Springer, Cham, pp. 1–16.

Blackburn, K., Green, D., 2021. The potential effects of microplastics on human health: what is known and what is unknown. *Ambio* 1–13.

Bondelind, M., Sokolova, E., Nguyen, A., Karlsson, D., Karlsson, A., Björklund, K., 2020. Hydrodynamic modelling of traffic-related microplastics discharged with stormwater into the Göta River in Sweden. *Environ. Sci. Pollut. R.* 27, 24218–24230.

Chen, H.L., Selvam, S.B., Ting, K.N., Gibbins, C.N., 2021. Microplastic pollution in freshwater systems in Southeast Asia: contamination levels, sources, and ecological impacts. *Environ. Sci. Pollut. R.* 28 (39), 54224–54237.

Chen, Y., Gao, B., Xu, D., Sun, K., Li, Y., 2022. Catchment-wide flooding significantly altered microplastics organization in the hydro-fluctuation belt of the reservoir. *iScience*, 104401.

Cheung, P.K., Hung, P.L., Fok, L., 2019. River microplastic contamination and dynamics upon a rainfall event in Hong Kong, China. *Environ. Process* 6 (1), 253–264.

De-la-Torre, G.E., 2020. Microplastics: an emerging threat to food security and human health. *J. Food Sci. Tech.* 57, 1601–1608.

Dong, L., Lin, L., Pan, X., Zhang, S., Lv, Z., Mi, C., 2022. Distribution Dynamics of Phthalate Esters in Surface Water and Sediment of the Middle-Lower Hanjiang River. *China Int. J. Env. Res. Pub. He.* 19, 2702.

Du, J., Xu, S., Zhou, Q., Li, H., Fu, L., Tang, J., Wang, Y., Peng, X., Xu, Y., Du, X., 2020. A review of microplastics in the aquatic environmental: distribution, transport, ecotoxicology, and toxicological mechanisms. *Environ. Sci. Pollut. R.* 27, 11494–11505.

Du, J., Zhou, Q., Li, H., Xu, S., Wang, C., Fu, L., Tang, J., 2021. Environmental distribution, transport and ecotoxicity of microplastics: a review. *J. Appl. Toxicol.* 41, 52–64.

- Eo, S., Hong, S.H., Song, Y.K., Han, G.M., Shim, W.J., 2019. Spatiotemporal distribution and annual load of microplastics in the Nakdong River, South Korea. *Water Res.* 160, 228–237.
- Eppehimer, D.E., Hamdhani, H., Hollien, K.D., Nemec, Z.C., Lee, L.N., Quanrud, D.M., Bogan, M.T., 2021. Impacts of baseflow and flooding on microplastic pollution in an effluent-dependent arid land river in the USA. *Environ. Sci. Pollut. R.* 28, 45375–45389.
- He, B., Smith, M., Egodawatta, P., Ayoko, G.A., Rintoul, L., Goonetilleke, A., 2021. Dispersal and transport of microplastics in river sediments. *Environ. Pollut.* 279, 116884.
- Hitchcock, J.N., 2020. Storm events as key moments of microplastic contamination in aquatic ecosystems. *Sci. Total. Environ.* 734, 139436.
- Hurley, R., Woodward, J., Rothwell, J.J., 2018. Microplastic contamination of river beds significantly reduced by catchment-wide flooding. *Nat. Geosci.* 11, 251–257.
- Junaaid, M., Liu, S., Liao, H., Liu, X., Wu, Y., Wang, J., 2022. Wastewater plastisphere enhances antibiotic resistant elements, bacterial pathogens, and toxicological impacts in the environment. *Sci. Total. Environ.*, 156805.
- Karbalaei, S., Hanachi, P., Walker, T.R., Cole, M., 2018. Occurrence, sources, human health impacts and mitigation of microplastic pollution. *Environ. Sci. Pollut. R.* 25, 36046–36063.
- Kataoka, T., Nihei, Y., Kudou, K., Hinata, H., 2019. Assessment of the sources and inflow processes of microplastics in the river environments of Japan. *Environ. Pollut.* 244, 958–965.
- Koutnik, V.S., Leonard, J., Alkidim, S., DePrima, F.J., Ravi, S., Hoek, E.M., Mohanty, S.K., 2021. Distribution of microplastics in soil and freshwater environments: global analysis and framework for transport modeling. *Environ. Pollut.* 274, 116552.
- Kumar, R., Sharma, P., Verma, A., Jha, P.K., Singh, P., Gupta, P.K., Chandra, R., Prasad, P.V., 2021. Effect of physical characteristics and hydrodynamic conditions on transport and deposition of microplastics in riverine ecosystem. *Water* 13, 2710.
- Li, J., Liu, H., Chen, J.P., 2018. Microplastics in freshwater systems: review on occurrence, environmental effects, and methods for microplastics detection. *Water Res.* 137, 362–374.
- Lu, X., Wang, X., Ban, X., Singh, V.P., 2020. Transport characteristics of non-cohesive sediment with different hydrological durations and sediment transport formulas. *J. Hydrol.* 591, 125489.
- Moriasi, D.N., Gitau, M.W., Pai, N., Daggupati, P., 2015. Hydrologic and water quality models: Performance measures and evaluation criteria. *Trans. ASABE* 58, 1763–1785.
- Niu, L., Li, Y., Li, Y., Hu, Q., Wang, C., Hu, J., Zhang, W., Wang, L., Zhang, C., Zhang, H., 2021. New insights into the vertical distribution and microbial degradation of microplastics in urban river sediments. *Water Res.* 188, 116449.
- Nizzetto, L., Bussi, G., Futter, M.N., Butterfield, D., Whitehead, P.G., 2016. A theoretical assessment of microplastic transport in river catchments and their retention by soils and river sediments. *Environ. Sci.: Process. Impacts* 18, 1050–1059.
- Noori, N., Kalin, L., 2016. Coupling SWAT and ANN models for enhanced daily streamflow prediction. *J. Hydrol.* 533, 141–151.
- Petersen, F., Hubbart, J.A., 2021. The occurrence and transport of microplastics: the state of the science. *Sci. Total. Environ.* 758, 143936.
- Rochman, C.M., 2018. Microplastics research—from sink to source. *Science* 360, 28–29.
- Sana, S.S., Dogiparthi, L.K., Gangadhar, L., Chakravorty, A., Abhishek, N., 2020. Effects of microplastics and nanoplastics on marine environment and human health. *Environ. Sci. Pollut. R.* 27, 44743–44756.
- Sharma, S., Chatterjee, S., 2017. Microplastic pollution, a threat to marine ecosystem and human health: a short review. *Environ. Sci. Pollut. R.* 24, 21530–21547.
- Talbot, R., Chang, H., 2022. Microplastics in freshwater: a global review of factors affecting spatial and temporal variations. *Environ. Pollut.* 292, 118393.
- Vethaak, A.D., Legler, J., 2021. Microplastics and human health. *Science* 371, 672–674.
- Waldschläger, K., Schüttrupf, H., 2019. Effects of particle properties on the settling and rise velocities of microplastics in freshwater under laboratory conditions. *Environ. Sci. Technol.* 53, 1958–1966.
- Wang, C., Zhao, J., Xing, B., 2021. Environmental source, fate, and toxicity of microplastics. *J. Hazard. Mater.* 407, 124357.
- Wang, J., Qin, X., Guo, J., Jia, W., Wang, Q., Zhang, M., Huang, Y., 2020. Evidence of selective enrichment of bacterial assemblages and antibiotic resistant genes by microplastics in urban rivers. *Water Res.* 183, 116113.
- Weideman, E.A., Perold, V., Ryan, P.G., 2019. Little evidence that dams in the Orange-Vaal River system trap floating microplastics or microfibres. *Mar. Pollut. Bull.* 149, 110664.
- Windsor, F.M., Durance, I., Horton, A.A., Thompson, R.C., Tyler, C.R., Ormerod, S.J., 2019. A catchment-scale perspective of plastic pollution. *Glob. Change Biol.* 25 (4), 1207–1221.
- Wu, P., Tang, Y., Dang, M., Wang, S., Jin, H., Liu, Y., Jing, H., Zheng, C., Yi, S., Cai, Z., 2020. Spatial-temporal distribution of microplastics in surface water and sediments of Maozhou River within Guangdong-Hong Kong-Macao Greater Bay Area. *Sci. Total. Environ.* 717, 135187.
- Xia, W., Rao, Q., Deng, X., Chen, J., Xie, P., 2020. Rainfall is a significant environmental factor of microplastic pollution in inland waters. *Sci. Total. Environ.* 732, 139065.
- Xu, D., Gao, B., Wan, X., Peng, W., Zhang, B., 2022. Influence of catastrophic flood on microplastics organization in surface water of the Three Gorges Reservoir, China. *Water Res.* 211, 118018.
- Zhao, M., Cao, Y., Chen, T., Li, H., Tong, Y., Fan, W., Xie, Y., Tao, Y., Zhou, J., 2022. Characteristics and source-pathway of microplastics in freshwater system of China: a review. *Chemosphere*, 134192.